Chapter 10: Off-Axis "Leith & Upatnieks" Holograms

Many of the shortcomings of in-line "Gabor" holograms have been overcome by going to an off-axis geometry that allows the various image components to be separated, and also allowed opaque subjects to be front-illuminated. These discoveries were made by Emmett Leith and Juris Upatnieks, working at the Radar and Optics Lab of the University of Michigan's Willow Run Laboratories. They were working on optical data processing for a highly secret new form of side-looking radar when they found that their images were three-dimensional; they had rediscovered Gabor's ideas about holography, as they quickly realized. Around 1962, the first commercial helium-neon lasers became available and Leith and Upatnieks started making more ambitious holograms, slowly moving the reference beam off to the side and dividing the laser beam to illuminate the object[1,2]. Finally, they made some holograms big enough (100 mm x 125 mm) to be visible with both eyes, and astonished everyone at the annual meeting of the Optical Society of America in 1964 with an incredibly vivid hologram of a brass model of a steam locomotive[3].

A typical setup is as shown in the margin. Most of the light goes through the beam-splitter to illuminate the object, and the diffusely reflected light, the "object beam," strikes the photo-sensitive plate. If that were all there were to it, we would just get a fogged plate. However, a relatively small amount of laser light is reflected off to be expanded to form the "reference beam," which overlaps the object beam at the plate to produce the holographic interference pattern. After exposure and processing, the plate (now called the "hologram") is put back in place, and illuminated with expanded laser light, usually with the same angle and divergence as the reference beam. Diffraction of the illumination beam produces several wavefront components, including one that reproduces the waves from the object—whence the 3-D image reconstruction. The various components are now separated by angles comparable to the reference beam angle, so that they no longer overlap and a clear window-like view of the scene is available.

Implications of off-axis holography: The dramatic increase of the angle between the reference and object beams has several important consequences:

separation of image terms-
Because there is a fairly large angle between the object and reference beam, the conjugate image will be well-separated from the true image, and may even be evanescent. Also, the straight-through beam, the zero-order component, will probably not fall into the viewer's eyes. The ability to clearly see a high-contrast, high-resolution image in vivid 3-D changed people's interest in holography literally overnight.

much finer fringes-
The large average angle means that the interference fringes will be much finer, typically more than 1000 fringes/mm^2. A typical photographic film can resolve details up to around 100 cy/mm^2, so ultra-fine-grained films are required for holography. Typical holographic materials have grains averaging 35 nm in diameter, compared to 1000 nm for conventional photo films (a volume ratio of one to 23,000!). Unfortunately, the sensitivity of emulsions drops quickly with decreasing grain size, and the equivalent ASA rating of the *8E75-HD* emulsion we use is about 0.001. That means that the exposure times will be quite long, usually up to ten seconds and sometimes much longer.

Another result is that the fringes will be closer to each other (a micron or so apart) than the emulsion layer is thick (five to seven microns, typically), so that volume diffraction effects can become noticeable. For the most part, this amounts to a modest sensitivity to the direction of illumination, but it also allows higher diffraction efficiencies to be reached with proper processing. At the same time, small defects in processing (especially during drying) become apparent if they cause mechanical shearing in the emulsion, and a distortion of the venetian-blind-like fringe structures.
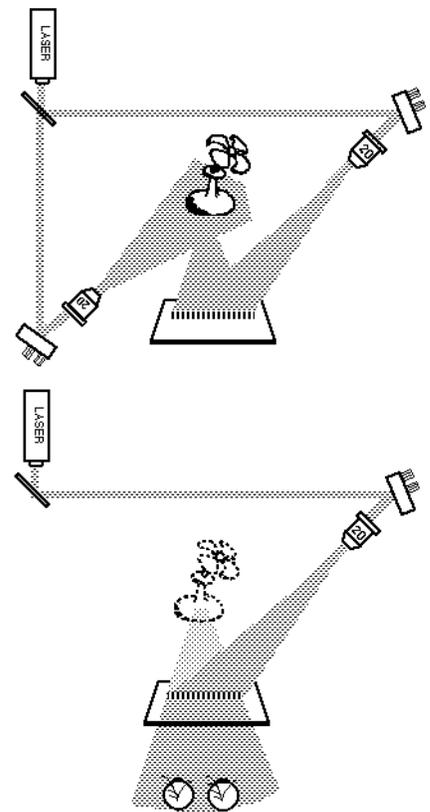
greater exposure stability required-
The finer fringes mean that the recording material must stand still to within
much higher tolerances during the exposure. And the lower sensitivity
(compared to lower resolution emulsions) means that those exposures will be
fairly long. In addition, because the beam paths are separated by the
beamsplitter, vibrations of the mirrors are not canceled out in the two beams, so
that the setup is more vulnerable to noise and shocks. Also, any element that is
reflecting a beam (including the object!) need move only one-quarter
wavelength to produce a shift of fringe position of one-half cycle, which washes
out the fringes during exposure.

frontal illumination of objects-
Two more issues come up because we are reflecting light from fairly deep
groups of ordinary diffusely-reflecting objects:

    coherence length:
If the lengths of the object and reference beam paths are matched for light
reflecting from the front of the object, they will be mismatched for light from
the rear by double the depth of the scene. This distance may be greater than the
"coherence length" of the light from the particular laser used, which may be
only a centimeter or two. Also, the steep reference beam angle means that the
length of the reference beam will also vary across the width of the plate.

    depolarization:
Interference happens only between similarly-polarized beams; the electric fields
have to be parallel in order to add or subtract. Diffuse reflection (such as from
matte paint) "scrambles" the polarization of a beam so that half of the object
light simply fogs the plate, and is lost to the holographic exposure.

beam ratio effects-
Because we can usually adjust the reflection:transmission "split ratio" of the
beamsplitter, we can adjust the ratio of the reference-to-object beam intensities,
K, to any number we desire. This allows us to increase the diffraction efficiency
of the hologram (the brightness of the image) more or less at will, up to the
maximum allowed by the plate and processing. Typically, we will use a K of
between 5 and 10. This will produce diffraction efficiencies of up to 20% with
"bleach" processing. However, as the object beam intensity is raised relative to
the reference beam (the K is lowered), additional noise terms arise caused by
object self-interference. They grow as the third power of the diffraction
efficiency, and reduction of the image contrast is often the practical limit on
reducing K. Also, because only a small fraction of the object light is captured
by the plate, increasing the beam split to the object increases light wastage, and
thereby increases the exposure time significantly. Long exposure times often
produce dim holograms, due to mechanical "creep" in the system, which defeats
the purpose of decreasing the K!

higher illumination bandwidth sensitivity:
Although going off-axis increases the sensitivity to source spectral bandwidth
(because we are seeing the spectral blur more nearly sideways), it also decreases
the sensisivity to vertical source size—a feature that will become useful with
white-light viewed holograms. However, it is only a $\cos\theta$ effect, which is not
very strong.

relation to in-line holography:
Careful observers in Lab #4 will have already noticed some of the features of
off-axis transmission holography near the edges of their in-line "Gabor"
holograms. At the edges of the plate, the angle between beams from the objects
and the unscattered reference beam is large enough to separate the various other
real and/or virtual images so that each may be seen more or less individually.
The price was a (likely) drop-off in diffraction efficiency corresponding to the
finer fringe pattern (recall that the table was not floating), and a greater blurring
in white-light viewing. If you imagine tilting a plate that is far from the ZFP of
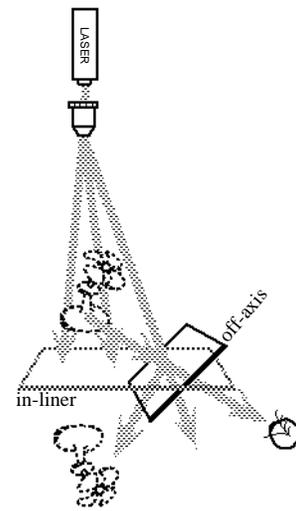
a Gabor hologram, you have an off-axis hologram (except for the beam-split separation of the reference beam and object illumination beam). So, there really are no new physics concepts involved here, but their implications become quite different.

Interference and diffraction in off-axis holograms

We should begin by going through the same process that we did for the on-axis hologram: examine the phase footprints of the two waves involved (with a single point serving as a "stand-in" for the 3-D object), and going on through the interference pattern and the transmittance, add the illumination, and examine the output terms for likely suspects. Instead, we will invoke the master phase equation of holography as a short-cut.

\

We begin by defining terms. The reference beam comes in at some angle (positive in this example, for convenience), and the object beam will be on axis. As a rule, the radius of curvature of the reference beam will be much larger than that of the object beam, but this need not necessarily be the case as long as the intensity of the reference beam is fairly uniform across the plate.
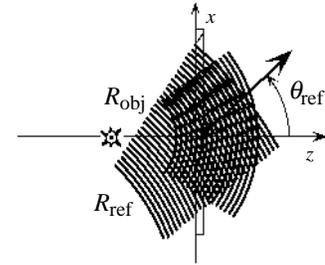
phase footprint of the output waves: __
The phase footprint (the first few terms, anyway) of an off-axis spherical wave was described in Chap. 9 (Eq. 3), and in the current vernacular translates to be:

$$\phi_{ref}(x,y) = \phi_0 + \frac{2\pi}{\lambda_1}\sin\theta_{ref}\ x + \frac{\pi}{\lambda_1}\left(\frac{\cos^2\theta_{ref}}{R_{ref}}x^2 + \frac{1}{R_{ref}}y^2\right). \qquad (1)$$

By comparison, the phase footprint of an on-axis point object wave should look familiar by now (note that $\cos^2\theta_{obj}=1$):

$$\phi_{obj}(x,y) = \phi_1 + \frac{\pi}{\lambda_1 R_{obj}}\left(x^2 + y^2\right). \qquad (2)$$

All that we lack is the illumination beam, which will again be an off-axis spherical wave, with a phase footprint of the same general form as the reference wave:

$$\phi_{ill}(x,y) = \phi_2 + \frac{2\pi}{\lambda_2}\sin\theta_{ill}\ x + \frac{\pi}{\lambda_2}\left(\frac{\cos^2\theta_{ill}}{R_{ill}}x^2 + \frac{1}{R_{ill}}y^2\right). \qquad (3)$$

Now we will invoke the fundamental phase-addition law of holography, first revealed in Ch. 7 ("Platonic Holography"):

$$\phi_{out,m}(x,y) = m\left(\phi_{obj}(x,y) - \phi_{ref}(x,y)\right)\phi_{ill}(x,y), \qquad (4)$$

where each of the output waves has its own angle of inclination and radius of curvature,

$$\phi_{out,m}(x,y) = \phi_3 + \frac{2\pi}{\lambda_2}\sin\theta_{out}\ x + \frac{\pi}{\lambda_2}\left(\frac{\cos^2\theta_{out}}{R_{out,x}}x^2 + \frac{1}{R_{out,y}}y^2\right). \qquad (5)$$

Now it is only necessary to separately match the coefficients of the linear terms in x, and the quadratic terms in x and y (we do not bother with the constant phase terms, of course). This produces the results that characterize the output wave:

$$\sin\theta_{out,m} = m\frac{\lambda_2}{\lambda_1}\left(\left(\sin\theta_{obj}=0\right)-\sin\theta_{ref}\right)+\sin\theta_{ill} \qquad (6)$$

$$\frac{\cos^2\theta_{out,m}}{R_{out,m,x}} = m\frac{\lambda_2}{\lambda_1}\left(\frac{1}{R_{obj}}-\frac{\cos^2\theta_{ref}}{R_{ref}}\right)+\frac{\cos^2\theta_{ill}}{R_{ill}} \qquad (7)$$

$$\frac{1}{R_{out,m,y}} = m\frac{\lambda_2}{\lambda_1}\left(\frac{1}{R_{obj}}-\frac{1}{R_{ref}}\right)+\frac{1}{R_{ill}} \qquad (8)$$

Note that these are just our familiar "$\sin\theta$" and "$1/R$" equations, plus a new addition, the "cosine-squared (over R)" equation for the radius of curvature of the output wave in the x-direction.

perfect reconstruction:
Note that if we again have $\lambda_2=\lambda_1$, $R_{\text{ill}}=R_{\text{ref}}$, and $m=+1$, we achieve "perfect reconstruction" in that $\theta_{\text{out}}=0°$, and $R_{\text{out,x}}=R_{\text{out,y}}=R_{\text{obj}}$. That is, the image will be located at the same place as the object, which will be true for every point in the object.
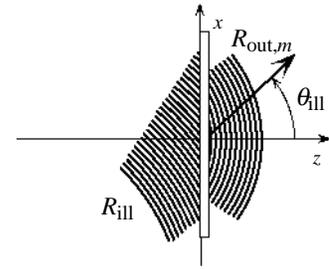
the conjugate image:
Let's leave everything about the illumination the same, but examine the $m=-1$ or "conjugate" image for a moment. Note that the output beam angle is now

$$\theta_{-1} = \sin^{-1}(2\sin\theta_{\text{ref}}), \qquad (9)$$

and does not exist if the reference beam angle is 30° or more (that is, the wave will be evanescent). This is the usual case in off-axis holography, as typical reference beam angles are 45° or 60°. We might deliberately make some shallow-reference-angle holograms just to make the conjugate image easier to see. Instead, we usually display the conjugate image by illuminating the hologram from the other side of the z-axis, with $\theta_{\text{ill}}\approx-\theta_{\text{ref}}$ (so that the conjugate image comes on-axis), or by more often by illuminating through the back of the plate, with $\theta_{\text{ill}}\approx\pi+\theta_{\text{ref}}$, (about which much more will be said in later chapters).

If the conjugate image exists at all, it is very likely to be a real image. Consider first the y-curvature (letting $\lambda_2=\lambda_1$ and $R_{\text{ill}}=R_{\text{ref}}$ and $\theta_{\text{ill}}=\pm\theta_{\text{ref}}$ for simplicity):

$$R_{-1,y} = -R_{\text{obj}}\left(\frac{\dfrac{R_{\text{ref}}}{R_{\text{obj}}}}{\dfrac{R_{\text{ref}}}{R_{\text{obj}}} - 2}\right). \qquad (10)$$

As long as the reference point is more than twice as far away as the object, the conjugate image will be real. Otherwise, it will be a virtual image, appearing beyond the illumination source. But consider now the x-curvature:

$$R_{-1,x} = -\cos^2\theta_{-1}\, R_{\text{obj}}\left(\frac{\dfrac{R_{\text{ref}}}{R_{\text{obj}}}}{\dfrac{R_{\text{ref}}}{R_{\text{obj}}} - 2\cos^2\theta_{\text{ref}}}\right). \qquad (11)$$

Note that it is, in general, very different from the y-curvature. It may even have a different sign! This is our first real taste of the dreaded *astigmatism*, which will plague us for the rest of the semester. It means that the rays that are converging to the point-like real-image focus will cross first in the x-direction, and later in the y-direction (as a rule). In general, we will have to treat the x- and y- focusing of the hologram separately at each step. Because the x-direction will often be vertical, we will call it the vertically-focused image (or *tangential* focus, in conventional lens-design terms). The y-focus is then the horizontally-focused image (or *sagittal* focus).

higher-order images:
Note that, if the $m=-1$ term is evanescent, the $m=+3$ term will usually be evanescent too, and all the higher-order terms (assuming that $\theta_{\text{out,+1}}\approx0°$). Some of those higher order terms can be brought into view by manipulating the illumination angle and/or wavelength. They will be formed closer to the hologram, just as for the in-line hologram, and follow the same rules (for the wavefront y-curvature, anyway).
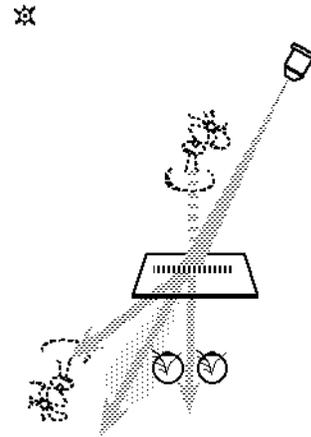
imperfect reconstruction—*astigmatism*! :

Considering again the $m=+1$ or "true" image, note that if the illumination wave is not a perfect replica of the reference wave (that is, it has a different wavelength, angle, or divergence), the output wave will not be a perfect replica of the spherical wave created by the point object. In fact, it will probably not be a spherical wave! For "imperfect" reconstructions, the radii of curvature in the x- and y-directions, given by Eqs. 7 & 8, will be different, often significantly so.

It is difficult to get used to thinking about astigmatic wavefronts and astigmatic ray bundles, and we will make several tries at making it clear. A wavefront with different curvatures in two perpendicular directions has a shape like that of the surface of a football where a passer usually grabs it (near the stitching). It has a small radius of curvature around the waist of the ball, and a long radius of curvature from end to end. If you try to focus such a wave onto a card to see what kind of source produced it, you would first see a vertical line, then a round circle, and then a horizontal line as you passed the card from the first center of curvature to the second. Many people have astigmatism in their eyes (usually from a cornea that is non-spherical) and have a cylindrical lens component in their prescription to allow a sharp focus to be restored.
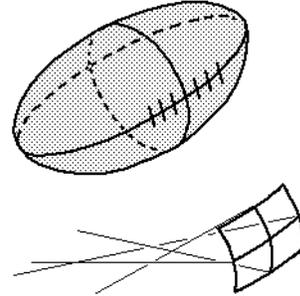
Thinking about it in ray terms, a point source produces a *stigmatic* ray bundle (from the Greek for pin-prick or tattoo mark), a bundle of rays that seem to have passed through a single point in space. Instead, an *astigmatic* (non-stigmatic) ray bundle seems to have passed through two crossed slits that are somewhat separated. The curvature in each of the two directions is equal to the distance to the perpendicular slit, and the rays have no common origin point.

We will struggle to visualize astigmatic ray bundles in class—no two-dimensional sketch can do the phenomenon justice! In addition to blurring a focused image, the usual visual effect is that the distance of an image seems to be different depending on the direction we move our head (side-to-side versus up-to-down).

Interestingly, there are some conditions of imperfect illumination that do not produce astigmatism. One condition that is easy to derive is obtained if the object and image are perpendicular to the plate and if

$$\frac{\sin^2 \theta_{\text{ill}}}{R_{\text{ill}}} = \frac{\sin^2 \theta_{\text{ref}}}{R_{\text{ref}}} \quad . \qquad (12)$$

Another case, of some practical interest later on, occurs when only the distance to the illumination source changes. If the object and image angles are equal and opposite to the reference and illumination angles (also equal), then there will be no astigmatism for any pair of reference and illumination distances! That is to say, all of the $\cos^2$ terms in Eq. 7 are equal, and so divide out.

If you are a photographer, you may also have come across lenses called *anastigmats*. That name comes from the Greek for "again" and "pin-prick" or "point-like," which is only to say that the lenses claim to produce a particularly sharp spherical-wave focus.

Astigmatism will be a much stronger effect when we deal with real image projection in a few chapters, and we will be studying it in some detail. For the time being, we will be content with the examples at the end of the chapter. Its effects in virtual image reconstruction are usually so weak as to be almost invisible, but it is important to understand astigmatism in principle, even now. Strangely, it is a subject that is not much discussed or appreciated in the holography literature, although researchers noted its existence early in the history of the field[4,5].

Models for off-axis holograms

The three equations that describe image formation by an off-axis hologram seem pretty opaque at first glance, although they will gradually become more familiar as the semester moves along. In the meantime, it is tempting to draw some simple physical models to describe the optical properties of off-axis holograms. We will look at two such models; the first is a deliberate "straw man,"

appealingly simple but hopelessly inaccurate. It can be used only for a very rough first judgement of physical reasonability.

<u>off-axis zone plate:</u>
We have seen that the off-axis hologram can be considered as an extreme case of an on-axis hologram, at least conceptually. Why, then, can't we apply the same model of a Gabor zone plate, using simple raytracing through key landmarks, such as the zero-frequency point, the ZFP? Such a model might look like the sketch, which shows a collimated illumination beam at 20°, which is presumably the same angle as the reference beam. If the object was 100 mm from the plate, the ZFP is 36.4 mm above the axis. The distance from the hologram to the real and virtual foci should be equal in collimated illumination, so the real image location is predicted to be $(x,z)=(72.8, 100)$. The more carefully calculated location is (68.4, 72.9), significantly different! What is the problem with the Gabor zone plate model now? Recall that our analysis assumed that the rays of interest travels close to and at small angles to the optical axis of the zone plate, what we called a "paraxial" analysis. But for an off-axis hologram, the rays of interest pass through the center of the hologram, which is far from the ZFP and the optical axis of the zone plate. The off-axis and large-angle aberrations have become too large to accurately predict anything but the location of the virtual image in near-perfect reconstruction.
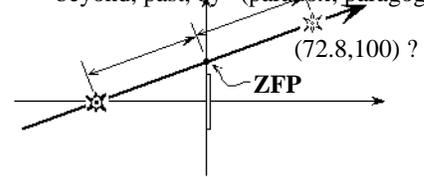
<u>prism + lens (grating + zone plate) model</u>
What the $\sin\theta$ and $1/R$ equations for the $m=+1$ image are telling us is that the light turns upon reaching the hologram, as though deflected by a diffraction grating (or its refractive equivalent, a base-down prism), and then is focused (well, diverged) by an on-axis Gabor zone plate (or its equivalent, a negative or double-concave lens). On the other hand, the $m=-1$ image is deflected the opposite way (the opposite order of the image, or a base-up prism) and focused by the opposite power of the zone plate (or its equivalent, a positive or double-convex lens). Higher order images are generated by prisms and lenses, each having multiples of the base power, always paired. Refracting elements seem to be more photogenic than their diffractive equivalents, so we often sketch an off-axis hologram as a combination of two lens-prism pairs (in idealized optics, it doesn't matter which comes first). Upon examination of the transmittance pattern, we find a constant spatial frequency term plus a term with a linearly varying frequency, which can be interpreted as two diffractive elements in tandem, exactly as suggested by these sketches. Thus this model brings us quite close to the mathematical as well as physical reality of off-axis holograms.
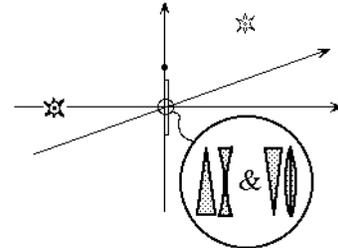
The focus in the x-direction is a little different, as there is some coupling between the power of the equivalent lens and the equivalent prism, so that the lens itself has different curvatures in the two directions, as would a lens designed to correct astigmatic vision. The appearance of an astigmatically focused image is difficult to describe. For an image focused on a card, vertical and horizontal lines will come into sharp focus at slightly different distances. An aerial image—viewed in space by an eye—may seem to have different magnifications in the two directions. The implications will be context-specific, so we will explore them as they arise in holographic imaging systems.

The $\sin\theta$ equation is exact; it is a raytracing equation after all. But the focusing equations are valid only for small variations of angle or location around the accurately raytraced component. We call this a "parabasal" type of analysis, one that is valid only in the mathematical vicinity of the "basal ray" that is traced through the part of the hologram of interest, even though that ray strays far from the z-axis and has several large-angle bends.

Image magnification
Now that we have found the image locations fairly accurately, all that remain to be found are the magnifications of the images to finish our characterization of off-axis holograms as 3-D imaging systems.

para- [1] 1. a prefix appearing in loanwords from Greek, with the meanings "at or to one side of, beside, side by side" (parabola; paragraph), "beyond, past, by" (paradox; paragoge).

<u>longitudinal magnification:</u>
Note that the "$1/R$" equation is the same for off-axis and on-axis holograms, and recall that this is the equation that governs longitudinal magnification. Thus the same equation (which followed from the derivative of the R_{out}) applies, but now re-stated in terms of wavefront curvatures:

$$MAG_{long} = \frac{\Delta R_{out,m}}{\Delta R_{obj}} = m\frac{\lambda_2}{\lambda_1}\left(\frac{R_{out,m}}{R_{obj}}\right)^2 . \qquad (13)$$

We only have to point out that the radii are now measured along a line through the center of the hologram and the center of the object, which may be at a large angle to the z-axis.

The x-focus or "$\cos^2$" equation moves the images around and changes their magnification. Discussion of the exact relationship is deferred to a later draft of these notes!

<u>lateral magnification:</u>
The angular subtense approach is the only workable handle on lateral magnification in this case, as the "ZFP & central ray" method is no longer applicable. Remembering the interference patterns caused by light from the top and bottom of an arrow some distance from the hologram, the marked tilt of the reference beam causes these two object beams to generate slightly different spatial frequencies. The subtense of the output rays is then determined by the difference in the output angles for those same frequencies. Recalling the discussion that led up to the final equation of the previous chapter, we have the lateral magnification expressed as

$$MAG_{lateral,x} = m\frac{\lambda_2}{\lambda_1}\frac{\cos\theta_{obj}}{\cos\theta_{out,m}}\frac{R_{out,m,x}}{R_{obj}} . \qquad (14)$$

This is the magnification in the x-direction, and requires knowledge of the corresponding image distance (or wavefront curvature). Diffraction in the y-direction is less clearly analyzed in our terms, but the angular subtense does not depend on the angles involved, so the corresponding equations follow as (tentatively—these have not yet been experimentally confirmed):

$$\frac{\Delta\theta_{out,m,y}}{\Delta\theta_{obj}} = m\frac{\lambda_2}{\lambda_1} ,$$

$$MAG_{lateral,y} = m\frac{\lambda_2}{\lambda_1}\frac{R_{out,m,y}}{R_{obj}} . \qquad (15)$$

Intermodulation noise

Another component of the light is what we have been calling "halo light," which is also called "intermodulation noise" and "object shape dependent noise." It produces a diffuse fan of light around the zero-order beam, the attenuated straight-through illumination beam. If the non-linearities in the emulsion response are very strong, it also causes diffuse light to appear in and around the image, but here we will concentrate on the halo of light around the zero-order beam, and find the conditions that will keep it from overlapping the image light. The key question is "what is the angle of the halo fan?"

The halo is caused by the interference of light from points on the object. We have been considering the hologram as though there were only one object point at a time. When there are many points (the usual case), coarse interference fringes arise from interference among them. Because the object points are all at roughly the same distance from the hologram, the gratings that "intra-object" interference produces are of approximately constant spatial frequency across the hologram. To find the limits of the fan of halo light, we only need to consider interference between the most widely spread object points. We designate the angle subtended by the object as $\Delta\theta_{obj}$. The maximum spatial frequency of the
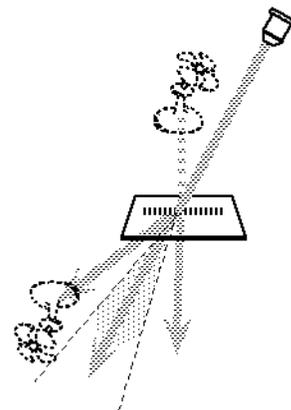
intra-object interference grating (f_{IMN}) is then, assuming that the center of the object is perpendicular to the plate,

$$f_{IMN} = \frac{2\sin\left(\dfrac{\Delta\theta_{obj}}{2}\right)}{\lambda_1} \ . \tag{16}$$

To avoid overlap of the halo light and the image light, it is only necessary that the minimum spatial frequency of the image gratings be greater than f_{IMN}. This relationship is expressed as

$$f_{obj-min} = \frac{\sin\theta_{ref} - \sin\left(\dfrac{\Delta\theta_{obj}}{2}\right)}{\lambda_1}$$

$$\geq \frac{2\sin\left(\dfrac{\Delta\theta_{obj}}{2}\right)}{\lambda_1} , \text{ or} \tag{17}$$

$$\sin\theta_{ref} \geq 3\sin\left(\frac{\Delta\theta_{obj}}{2}\right).$$

Thus the size, or rather the angular subtend, of an object is limited by the choice of reference beam angle, if the overlap of halo light is to be avoided. If the object has an angular subtend of 30°, for example, then the reference beam angle must be at least 51°. The intensity of halo light drops off smoothly from the center to the edges of the fan, so these limitations can be stretched a bit before much image degradation is visible. However, there are several other sources of scatter that can send illumination beam light into the image area, so that controlling halo is only one issue to pay attention to.
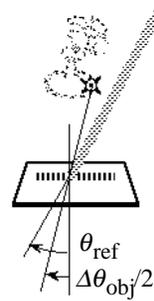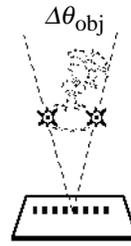
Conclusions

Off-axis holograms may require three times as many equations as diffraction gratings, but they involve the same physical principles and fit in the same logic that we started developing several weeks ago. Compared to in-line holograms, they require one new equation, the "cos-squared" focusing law that describes the *astigmatism* of off-axis holographic imaging. Astigmatism has minimal implications for virtual images, but will soon have to be dealt with very carefully for real images. In exchange for this mathematical complexity, we have moved into the domain of holograms that produce truly impressive three images!

References:
1. E.N. Leith and J. Upatnieks, "Reconstructed wavefronts and communication theory,"
   J. Opt. Soc. Amer. **52**, pp. 1123-30 (1962).
2. E.N. Leith and J. Upatnieks, "Wavefront reconstruction with continuous-tone objects,"
   J. Opt. Soc. Amer. **53**, pp. 1377-81 (1963).
3. E.N. Leith and J. Upatnieks, "Wavefront reconstruction with diffused illumination and three-dimensional objects,"
   J. Opt. Soc. Amer. **54**, pp. 1295-1301 (1964).
   That famous "Train and Bird" hologram is on display at the MIT Museum.
4. R.W. Meier, "Magnification and third-order aberrations in holography,"
   J. Opt. Soc. Amer. **55,** pp. 987-992 (1965).
5. A.A. Ward and L. Solymar, "Image distortions in display holograms,"
   J. Photog. Sci. **24**, pp. 62-76 (1986).